THE JOURNAL OF BIOLOGICAL CHEMISTRY VOL. 288, NO. 16, pp. 11334–11347, April 19, 2013

A Novel P_{1B}-type Mn^{2+}-transporting ATPase Is Required for Secreted Protein Metallation in Mycobacteria*

Received for publication, December 22, 2012, and in revised form, March 11, 2013 Published, JBC Papers in Press, March 12, 2013, DOI 10.1074/jbc.M112.448175

Teresita Padilla-Benavides[‡1], **Jarukit E. Long**[§1], **Daniel Raimunda**[‡], **Christopher M. Sassetti**[§¶], **and José M. Argüello**[‡2]

From the [‡]*Department of Chemistry and Biochemistry Worcester Polytechnic Institute, Worcester, Massachusetts 01609, the* [§]*Department of Microbiology and Physiological Systems, University of Massachusetts Medical School, Worcester, Massachusetts 01655, and* [¶]*Howard Hughes Medical Institute, Chevy Chase, Maryland 20815*

Background: CtpC is an uncommon metal transport ATPase required for *Mycobacterium tuberculosis* virulence.
Results: CtpC shows Mn^{2+}-ATPase activity. Mutations in *ctpC* alter Mn^{2+} homeostasis, increase sensitivity to redox stress, and decrease Mn-superoxide dismutase activity.
Conclusion: CtpC is a Mn^{2+} transport ATPase required for homeostasis and the assembly of secreted metalloproteins in mycobacterium.
Significance: CtpC provides a novel mechanism for Mn^{2+} metallation of secreted proteins.

Transition metals are central for bacterial virulence and host defense. P_{1B}-ATPases are responsible for cytoplasmic metal efflux and play roles either in limiting cytosolic metal concentrations or in the maturation of secreted metalloproteins. The P_{1B}-ATPase, CtpC, is required for *Mycobacterium tuberculosis* survival in a mouse model (Sassetti, C. M., and Rubin, E. J. (2003) Genetic requirements for mycobacterial survival during infection. *Proc. Natl. Acad. Sci. U.S.A.* 100, 12989–12994). CtpC prevents Zn^{2+} toxicity, suggesting a role in Zn^{2+} export from the cytosol (Botella, H., Peyron, P., Levillain, F., Poincloux, R., Poquet, Y., Brandli, I., Wang, C., Tailleux, L., Tilleul, S., Charriere, G. M., Waddell, S. J., Foti, M., Lugo-Villarino, G., Gao, Q., Maridonneau-Parini, I., Butcher, P. D., Castagnoli, P. R., Gicquel, B., de Chastellièr, C., and Neyrolles, O. (2011) Mycobacterial P_1-type ATPases mediate resistance to zinc poisoning in human macrophages. *Cell Host Microbe* 10, 248–259). However, key metal-coordinating residues and the overall structure of CtpC are distinct from Zn^{2+}-ATPases. We found that isolated CtpC has metal-dependent ATPase activity with a strong preference for Mn^{2+} over Zn^{2+}. *In vivo*, CtpC is unable to complement *Escherichia coli* lacking a functional Zn^{2+}-ATPase. Deletion of *M. tuberculosis* or *Mycobacterium smegmatis ctpC* leads to cytosolic Mn^{2+} accumulation but no alterations in other metals levels. Whereas *ctpC*-deficient *M. tuberculosis* is sensitive to extracellular Zn^{2+}, the *M. smegmatis* mutant is not. Both *ctpC* mutants are sensitive to oxidative stress, which might explain the Zn^{2+}-sensitive phenotype of the *M. tuberculosis ctpC* mutant. CtpC is a high affinity/slow turnover ATPase, suggesting a role in protein metallation. Consistent with this hypothesis, mutation of CtpC leads to a decrease of Mn^{2+} bound to secreted proteins and of the activity of secreted Fe/Mn-superoxide dismutase, particularly in *M. smegmatis*. Alterations in the assembly of metalloenzymes involved in redox stress response might explain the sensitivity of *M. tuberculosis ctpC* mutants to oxidative stress and growth and persistence defects in mice infection models.

Transition metals are essential for life; however, at high concentrations, they can become toxic due to either adventitious metal binding to various biomolecules or the promotion of oxidative stress through Fenton chemistry (1, 2). To prevent metal toxicity, chaperone and chelating molecules tightly bind free ion species, and transmembrane transporters prevent excess accumulation in the cytosol. Together, these mechanisms maintain the aqueous milieu essentially free of uncomplexed metals (3–5). As a consequence of tightly regulated metal homeostasis, metalloproteins acquire the necessary cofactors through specific protein-protein interactions (4).

The involvement of transition metals in host-pathogen interaction is highlighted by the requirement of various transition metal transporters as well as transition metal-responsive transcriptional regulators for bacterial virulence (3, 6). Intracellular pathogens, such as *Mycobacterium tuberculosis*, must cope with transition metal starvation or excess stress during infection. For example, the natural resistance-associated macrophage protein 1 (Nramp1), a divalent cation-proton antiporter, participates in bacterial killing by driving Fe^{2+} efflux from the phagosome and starving the enclosed bacteria of this essential nutrient (7). Whether or not transition metals other than Fe^{2+} are depleted in the phagosome after infection is unclear (8, 9). In addition to the transition metal starvation model, it has been proposed that transporter recruitment to the phagosomal membrane may generate stress by increasing the concentration of free transition metal, such as Cu^{+} and Zn^{2+} (9–11). In particular, there is evidence that Zn^{2+} accumulation during infection hampers the growth of intracellular pathogens (11). Supporting this, expression of the lysosome-associated Zn^{2+} transporter ZIP8 in IFNγ-stimulated macrophages and T-cells has been reported (12, 13).

Transition metals also appear to be relevant for bacterial virulence through their participation in redox detoxification by

* This work was supported, in whole or in part, by National Institutes of Health Grant 1R21AI082484-01 (to J. M. A.) and Award F32A1093049 (to J. E. L.).
[1] Both authors contributed equally to this work.
[2] To whom correspondence should be addressed: Dept. of Chemistry and Biochemistry, Worcester Polytechnic Institute, 100 Institute Rd., Worcester, MA. Tel.: 508-831-5326; Fax: 508-831-4116; E-mail: arguello@wpi.edu.

metalloenzymes. For instance, *M. tuberculosis* survives in a highly oxidative environment by means of intracellular and secreted superoxide dismutases that participate in reactive oxygen species and reactive nitrogen species detoxification mechanisms (14–16). *M. tuberculosis* SodA, is a secreted Fe^{2+}/Mn^{2+}-dependent superoxide dismutase protein, but under *in vitro* growth conditions, it contains Fe^{2+} as a primary cofactor (14, 16, 17). SodA is exported in an unfolded state via a Sec-dependent mechanism (18), probably acquiring its metal cofactor in the extracytoplasmic milieu.

Heavy metal transport P_{1B}-ATPases[3] drive the efflux of a range of cytoplasmic metal ions, such as Cu^{+}, Zn^{2+}, and Co^{2+}, using the energy of ATP hydrolysis and are involved in maintaining cellular metal quotas (3, 19). The metal specificity of most P_{1B}-ATPase can be predicted based on the conserved signature sequences present in transmembrane segments 6, 7, and 8 (TM6, TM7, and TM8)[4] (3, 19–23). There are seven transition metal-transporting P_{1B}-ATPases in *M. tuberculosis* (20). Their signature transmembrane metal binding sites indicate that three (CtpA (cation transporter protein A), CtpB, and CtpV) are Cu^{+}-ATPases and that two others are likely Co^{2+}-ATPases (CtpD and CtpJ), whereas CtpC and CtpG appear to be novel transition metal transporters. Large scale genetic screens have predicted that *ctpC* and *ctpD* are specifically required for the optimal *in vivo* growth or survival of *M. tuberculosis* in the mouse model of tuberculosis (24). Microarray analyses of immune response induced genes have shown that *ctpC* and *ctpV* are expressed more robustly during infection of BALB/C mice than in the immune-defective SCID mouse strain or during *in vitro* growth (25). Similarly, induction of *ctpC*, *ctpG*, and *ctpV* in *M. tuberculosis* during macrophage infection has been reported (26). Linking CtpC activity with metal homeostasis during infection, early studies on *M. tuberculosis* Fe^{2+}-regulated genes showed that *ctpC* expression was induced in low Fe^{2+} medium (27).

Recently, Botella *et al.* (11) have shown that Zn^{2+} exposure induces the expression of *ctpC* and that a *ctpC*-null strain is hypersensitive to Zn^{2+} *in vitro*. *A priori*, these phenotypic characteristics might suggest that CtpC is a Zn^{2+}-ATPase. However, CtpC is structurally distinct from Zn^{2+}-transporting ATPases (20) because some of the invariant Zn^{2+}-coordinating residues involved in transmembrane translocation are absent from this protein. In addition, CtpC also lacks characteristic, although nonessential, regulatory cytoplasmic metal binding domains. These observations suggested that further characterization was necessary to define the biochemical function of this protein. We reexamined CtpC catalytic activity and its role in bacterial virulence to identify the substrate and consequent physiological role of this ATPase. Our results indicate that CtpC is a high affinity, slow turnover Mn^{2+}-ATPase, which is required for *M. tuberculosis* virulence. CtpC appears involved in the loading of Mn^{2+} into secreted metalloproteins, such as SodA. We propose that this function may be required for infection.

EXPERIMENTAL PROCEDURES

Bioinformatics Analysis—M. tuberculosis CtpC protein sequence was used for a BLAST search against all predicted sequence in the NCBI database. Among the returned hits, we selected those protein sequences lacking cytoplasmic metal binding domains (N- or C-MBD) and containing conserved transmembrane signatures, TM6 (CPC) and TM8 (H*XX*SS), probably involved in metal coordination during transport (20). Resulting homologous sequences were aligned with MUSCLE (28), Bioedit (29), and ESPript software (30). NCBI GI accession numbers were obtained, and the KEGG database nomenclature was used. The proteins that were not on KEGG were named with a three-letter key to denote the organismal origin as indicated in Fig. 1.

Bacterial Strains—M. tuberculosis H37Rv and *Mycobacterium smegmatis* $mc^{2}155$ cells were used in these studies. These were grown at 37 °C in 7H9 and 7H10 media (BD Biosciences) supplemented with 10% OADC (oleic acid, albumin, dextrose, catalase) enrichment or in Sauton's medium, as indicated in the figures. *Escherichia coli* BL21 (DE3) pLysS cells transformed with the plasmid pSJS1240 coding for rare tRNA (31) were grown at 37 °C in 2XYT medium containing 50 μg/ml spectinomycin, 34 μg/ml chloramphenicol.

ctpC Cloning and Expression—The *ctpC* gene was amplified from *M. tuberculosis* H37Rv and *M. smegmatis* $mc^{2}155$ genomic DNA using the primers Mtb *ctpC* Fwd plus Mtb *ctpC* Rvs and *ctpC*_smeg Fwd plus *ctpC*_smeg Rvs (Table 1). These introduced a tobacco etch virus protease site-coding sequence at the amplicon 3′-ends. The resulting amplicons were cloned into pBAD TOPO/His vector (Invitrogen) that introduces a C-terminal His_6 tag suitable for Ni^{2+} affinity purification. The *M. tuberculosis ctpC* cDNA was used as a template to introduce the mutations coding for single substitution H697A and double substation S700A/S701A, employing the QuikChange site-directed mutagenesis kit (Stratagene). The primers used are listed in Table 1. Sequences were confirmed by automated DNA sequence analysis. *E. coli* BL21 (DE3) pLysS pSJS1240 cells were transformed with these constructs and grown at 37 °C in 2XYT medium supplemented with 100 μg/ml ampicillin, 50 μg/ml spectinomycin, and 34 μg/ml chloramphenicol. Protein expression was induced with 0.002% L-arabinose. Cells were harvested 4 h after induction; washed with 25 mM Tris, pH 7.0, and 100 mM KCl; and stored at −80 °C. In alternative experiments, pBAD TOPO vector carrying *M. tuberculosis ctpC* was introduced in *E. coli* W3110 Δ*zntA* cells (32) and selected with 100 μg/ml ampicillin, 50 μg/ml kanamycin.

Protein Purification—CtpC purification was performed according to Mandal *et al.* (33). All purification steps were carried out at 0–4 °C. Cells were suspended in buffer A (25 mM Tris, pH 7.0, 100 mM sucrose, 1 mM phenylmethylsulfonyl fluoride (PMSF; Sigma)) and disrupted with a French press at 20,000 p.s.i. Lysed cells were centrifuged at 8,000 × *g* for 30 min. The supernatant was then centrifuged at 229,000 × *g* for 1 h, and the pelleted membranes were resuspended in buffer A (10–15 mg/ml). For protein solubilization and purification,

[3] For simplicity, P-type ATPases are referred to as P-ATPases, P_{1B}-ATPases, etc.
[4] The abbreviations used are: TM, transmembrane segment; N- and C-MBD, N- and C-terminal cytoplasmic metal binding domain, respectively; CBB, Coomassie Brilliant Blue; DDM, dodecyl-β-D-maltoside; qPCR, quantitative PCR; TEMED, *N*,*N*,*N*′,*N*′-tetramethylethylenediamine.

membranes were diluted to a final concentration of 3 mg/ml in buffer B (25 mM Tris, pH 8.0, 100 mM sucrose, 500 mM NaCl, 1 mM PMSF) and solubilized with 0.75% dodecyl-β-D-maltoside (DDM; Calbiochem). The preparation was incubated for 1 h at 4 °C with mild agitation and centrifuged at 229,000 × *g* for 1 h. The supernatant was incubated overnight at 4 °C with Ni^{2+}-nitrilotriacetic acid resin (Qiagen) pre-equilibrated with buffer B, 0.05% DDM, and 5 mM imidazole. The resin was washed with buffer B, 0.05% DDM containing 10 and 20 mM imidazole, and the protein was eluted with buffer B, 0.05% DDM, 250 mM imidazole. Fractions were pooled and concentrated, and buffer was replaced by 25 mM Tris, pH 8.0, 100 mM sucrose, 50 mM NaCl, and 0.01% DDM (buffer C) using 50 kDa cut-off centricons (Millipore). The proteins were aliquoted and stored in 20% (v/v) glycerol at −20 °C until use. All protein determinations were performed in accordance with the Bradford method (34). Purified CtpC protein was analyzed by 10% SDS-PAGE followed by Coomassie Brilliant Blue (CBB) staining or Western blot using an anti-His_6 tag antibody (GenScript).

ATPase Assays—The ATPase activity assay mixture contained 50 mM Tris, pH 6.8, 3 mM $MgCl_2$, 3 mM ATP, 0.01% asolectin, 0.01% DDM, 200 mM NaCl, 0.005 mg/ml purified CtpC, and either $MnCl_2$, $CuSO_4$, $ZnSO_4$, $CdCl_2$, $FeCl_3$, $NiCl_2$, or $CoCl_2$, as indicated in Fig. 2. ATPase activity was measured for 20 min at 37 °C. Released P_i was measured (35). Curves of ATPase activity *versus* Ag^+, Cu^+, or ATP, as well as enzyme phosphorylation curves, were fit to $v = V_{max} L/(L + K_{½})$, where L is the concentration of variable ligand. The reported S.E. values for V_{max} and $K_{½}$ are asymptotic S.E. values reported by the fitting software, KaleidaGraph (Synergy).

Recombineering, Mutant, and Complemented Strain Preparation—The *M. smegmatis ctpC* mutant strain was constructed following the procedures described previously (36, 37). For mutation of *M. tuberculosis ctpC*, a 1000-bp fragment corresponding to the 500 5′-most and 500 3′-most bp of *ctpC* was constructed. An insertion cassette containing the restriction sites for NotI-HpaI-AscI was added between the 5′- and 3′-most 500-bp regions. The resulting synthesized fragment was then inserted between HindIII sites in a pUC57 expression vector (GeneScript), resulting in plasmid pEL1a. Vector pKM342 contains a hygR cassette flanked by NotI-AscI sites. To insert the hygR cassette in pEL1a, both pEL1a and pKM342 were digested with NotI-AscI. The 1.2-kbp hygromycin fragment was then ligated into pEL1a, resulting in pEL2a. To generate the *ctpC* mutant, the resulting 2.2-kbp *ctpC-hygR-ctpC* fragment from digestion of pEL2a with HindIII was transformed into the *M. tuberculosis* H37Rv recombineering strain. Briefly, the *M. tuberculosis* H37Rv recombineering strain bearing plasmid pNIT:ET (38) was induced for 18 h with 1 μM isovaleronitrile. The culture was treated with 0.2 M glycine for 8 h before making electrocompetent cells and transformed. After selection on 7H10 plates containing hygromycin (50 μg/ml), the presence of the *ctpC* insertional mutation was assayed by PCR amplification of the hygR cassette flanked by the N- and C-terminal junctions. All primers used are listed in Table 1.

Constructs for mutant complementation assays were made by amplifying the *M. tuberculosis* and *M. smegmatis ctpC* from genomic DNA. The resulting PCR fragments were digested and ligated into pJEB402 (39), resulting in pJEB402-tbC and pJEB402-smC. The ligation reactions were transformed into DH5α cells, and the presence of the insert was verified by colony PCR and restriction digests. The plasmids were then purified and transformed into the mutant strains. Transformants showing kanamycin resistance were analyzed for the presence of the genes by PCR.

Metal and Redox Stressor Sensitivity Assays—*M. tuberculosis* H37Rv wild type, *ctpC*::*hyg*, and complemented strains were grown in 7H9-OADC medium to $A_{600} = 1.0$. Metal sensitivity was assayed by spotting dilution series of wild type, *ctpC*::*hyg*, and complemented strains on 7H10-OADC agar containing increasing concentrations of $CuCl_2$, $CoCl_2$, $MnCl_2$, $ZnSO_4$, or $CdCl_2$. For *tert*-butyl hydroperoxide sensitivity, 7H10-OAD was used instead of 7H10-OADC. Colony-forming units (CFU) were assessed after 18 days of incubation at 37 °C. *M. smegmatis* mc^2155 wild type, *ctpC*::*hyg*, and complemented strains were grown in 7H9-OADC medium with increasing concentrations of $ZnSO_4$ or $MnCl_2$. A_{600} was determined after 48 h of culture. For analyzing the sensitivity to extracellular redox stress, these strains were grown in 7H9 medium until $A_{600} = 1.0$. The cells were incubated for 0 (before addition), 30, 60, 90, and 120 min with 0.1 unit/ml xanthine oxidase and 250 μM hypoxanthine (Sigma) diluted 1:100 in phosphate-buffered saline as described previously (40). Serial dilutions were plated at different time points, and CFU were quantified. The percentage of survival (CFU at 30–120 min/CFU at 0 min) was calculated for three independent experiments.

Gene Expression Analysis—*M. tuberculosis H37*Rv and *M. smegmatis* mc^2155 cells in exponential phase were supplemented with 100 μM various metals and redox stressors as indicated in Figs. 4 and 5 and incubated for 2 h. Chelexed Sauton's medium was used to evaluate *ctpC* expression under metal starvation conditions. Sauton's medium, pH 7.4, containing 6% (v/v) glycerol, 3.6 mM KH_2PO_4, 11.4 mM citric acid, 30 mM asparagine, 0.1 μM $FeCl_3$, 4.2 mM $MgCl_2$, and 0.05% (v/v) Tween 80 was incubated overnight at 4 °C in constant stirring, in the presence (chelexed medium) or the absence (non-chelexed medium) of 1 g of Chelex beads (Sigma) per 100 ml of medium. Subsequently, 0.1 μM $FeCl_3$ and 4.2 mM $MgCl_2$ were added to the media. Manganese content was determined in 7H9, non-chelexed, and chelexed Sauton's media by furnace atomic absorption spectroscopy (Varian SpectrAA 880/GTA 100). 7H9 medium contained 0.88 ± 0.02 nM, non-chelexed Sauton's medium contained 0.36 ± 0.01 nM, and chelexed Sauton's medium contained 0.27 ± 0.01 nM Mn^{2+}. Cells were pelleted and rinsed three times with chelexed medium and incubated 2 h with either 7H9 or non-chelexed Sauton's medium as controls and chelexed Sauton's medium. Cells were harvested, resuspended in 1 ml of TRIzol reagent (Invitrogen), and disrupted using lysing matrix B (MP Biomedicals) in a cell disrupter (FastPrep FP120, Qbiogene). RNA pellets were air-dried and redissolved in 50 μl of diethyl pyrocarbonate-treated ultrapure water. The remaining DNA was removed with the RNeasy minikit and an on-column DNase I kit (Qiagen). The RNA samples (1 μg) were used as templates for cDNA synthesis with random primers and SuperScript III reverse transcriptase

TABLE 1
List of primers used in this study

Primer name	Sequence 5′–3′	Use
Mtb Fwd *ctpC*::*hyg* hygN-out2	5′-ACCAGTGCTCGCCGAACAGCTTGA-3′	Amplification of the N- terminal regions of Mtb *ctpC*
Mtb Rvs *ctpC*::*hyg* CatC-out2	5′-TGCACGGGACCAACACCTTCGTGG-3′	Amplification of the C-terminal regions of Mtb *ctpC*
prEL8	5′-TCGTTAACGACCCGGAAGAAAGGTACAG-3′	Amplification of the *M. tuberculosis* rv3269-ctpC operon
prEL9	5′-ATGGTACCCGAACGGCTGGTGGATTGAC-3′	Amplification of the *M. tuberculosis* rv3269-ctpC operon
Mtb *ctpC* Fwd	5′-ACCCTGGAAGTGGTATCGGACGCG-3′	Clone Mtb *ctpC* in pBAD
Mtb *ctpC* Rvs	5′-GCGGTCCAGGCGGTAGCGGAT-3′	Clone Mtb *ctpC* in pBAD
Mtb ctpC ANASS Fwd	5′-GCGGCGATCCTGGCTAACGCGTCGTCG-3′	Mutation of the TM-MBD (TM8) of Mtb *ctpC*
Mtb ctpC ANASS Rvs	5′-CGACGACGCGTTAGCCAGGATCGCCGC-3′	Mutation of the TM-MBD (TM8) of Mtb *ctpC*
Mtb ctpC HNAAA Fwd	5′-GCGATCCTGCACAACGCGGCTGCTGTGGCGGTGGTG-3′	Mutation of the TM-MBD (TM8) of Mtb *ctpC*
Mtb ctpC HNAAA Fwd	5′-CACCACCGCCACAGCAGCCGCGTTGTGCAGGATCGC-3′	Mutation of the TM-MBD (TM8) of Mtb *ctpC*
Mtb qFwd *sigA*	5′-CTCGGTTCGCGCCTACCTCA-3′	*M. tuberculosis* Housekeeping gene for qPCR analysis
Mtb qRvs *sigA*	5′-GCGCTCGCTAAGCTCGGTCA-3′	*M. tuberculosis* Housekeeping gene for qPCR analysis
Mtb qFwd *ctpC*	5′-TCGACGCCATCGTGTTCG-3′	*M. tuberculosis ctpC* gene for qPCR analysis
Mtb qRvs *ctpC*	5′-CTCGGGCTCCCAATCTTTATGC-3′	*M. tuberculosis ctpC* gene for qPCR analysis
Smeg6058-F	5′-GTGGCTGATCTGACGGTCGTATCCGACGCG GCCGGCCGCATGCGCG TACACGGCCGCTCTAGAACTAGTGGA-3′	Hyg cassette amplification with 50 bp of 5′-flanking region locus MSMEG_6058 added to the 5′-end
Smeg6058-R	5′-CTAGTCGATTTCGTACCGGATCAGCCGGGCG CTGTTGGCCACCACCGCAACATGCCTGCAGGTCGACTCT-3′	Hyg cassette amplification with 50 bp of 3′-flanking region locus MSMEG_6058 added to the 3′-end
MSMEG_6058-F	5′-CATAGGTGAGGAAGTGCCGCCGCCCGCCGC GGGCGACGCCGGCCACGACCACGACCACTGAGTGACCACTGAGTACCG TGGCTGATCTGACGGT CGT-3′	Hyg cassette amplification with 125 bp of 5′-flanking region locus MSMEG_6058 added to the 5′-end
MSMEG_6058-R	5′-GGCGGCCGACATGGTGAACGCGCCGGTGGG CGGTACGACGACGTGT TGCACACCGGCAGCGTTCGCCGAACGCCCTAGTCGATTTCGTACC GGA-3′	Hyg cassette amplification with 125 bp of 3′-flanking region locus MSMEG_6058 added to the 3′-end
intSmeg6058-For	5′-TTGATTCTCTTGGGGATTCG-3′	Deletion MSMEG_6058 verification
intSmeg6058-Rev	5′-ATGATGCGACCTATGGTGGT-3′	Deletion MSMEG_6058 verification
Smeg6058-V1	5′-GTGATGGCAGAGGCGCGCGAA-3′	Deletion MSMEG_6058 verification
Smeg6058-V2	5′-GTCAAGCGAATCGGCCGCCAC-3′	Deletion MSMEG_6058 verification
Fwd EcoRI ctpc	5′-ACTGGAATTCGTGGCTGATCTGACGGTCGT ATC-3′	Clone SMEG_6058 in pJEB402
Rvs HpaI ctpc	5′-ACTGGTTAACCTAGTCGATTTCGTACCGG-3′	Clone SMEG_6058 in pJEB402
ctpC_smeg fwd	5′-GTGGCTGATCTGACGGTCGTATC-3′	Clone SMEG_6058 in pBAD
ctpC_smeg rvs	5′-CTAGTCGATTTCGTACCGGATCAG-3′	Clone SMEG_6058 in pBAD
Msm_2758 qFwd *sigA*	5′-GAAGACACCGACCTGGAACT-3′	*M. smegmatis* Housekeeping gene for qPCR analysis
Msm_2758 qRvs *sigA*	5′-GACTCTTCCTCGTCCCACAC-3′	*M. smegmatis* Housekeeping gene for qPCR analysis
Msm qFwd *ctpC*	5′-CGTGGTGGCCCTTACGGTTC-3′	*M. smegmatis ctpC* gene for qPCR analysis
Msm qRvs *ctpC*	5′-CGATCGCAACCTGCTCGTGT -3′	*M. smegmatis ctpC* gene for qPCR analysis

(Invitrogen). Quantitative RT-PCR was performed with iQ SYBR Green supermix (Bio-Rad). Transcript analysis of *ctpC* was performed by quantitative RT-PCR with the primers listed in Table 1 with cycler conditions as described previously (41). The RNA polymerase σ factor (*sigA*) was used as an internal reference. Determinations were carried out with RNA extracted from three independent biological samples, with the threshold cycle (C_t) determined in triplicate. The relative levels of transcription were calculated by using the $2^{-\Delta\Delta}C_t$ method (42). The mock reverse transcription reactions, containing RNA and all reagents except reverse transcriptase, confirmed that the results obtained were not due to contaminating genomic DNAs (data not shown).

Metal Content Analysis—Whole cell metal contents were measured in *M. tuberculosis* strains grown to the late exponential phase and incubated in the presence or absence of 100 μM $ZnSO_4$ for 1 h. Metals bound to *M. tuberculosis* secreted proteins were measured in strains grown in Sauton's medium for 2 weeks at 37 °C. Cells were pelleted, and the supernatant was filtered through 0.2-μm filters (Corning Inc.) and concentrated using 3 kDa cut-off centricons (Millipore). Protein content was determined, and samples were prepared for metal content analysis. In the case of *M. smegmatis* metal-bound secreted proteins, cells were grown for 48 h in the presence or absence of 50 μM $MnCl_2$ and pelleted, and supernatants were processed as described above. To obtain cytosolic and membrane fractions, cells were grown as described and disrupted in a French press at 20,000 p.s.i., and homogenates were centrifuged at 8,000 $\times$ *g* for 30 min. Supernatant was centrifuged at 229,000 $\times$ *g* for 1 h. The supernatant of this centrifugation was considered the cytosolic fraction and concentrated with 3 kDa cut-off centricons. The pelleted membrane fractions were resuspended in 25 mM Tris, pH 7.0, 100 mM KCl, and protein content was determined.

All samples were acid-digested with HNO_3 (trace metal grade) for 1 h at 80 °C and overnight at 20 °C. Digestions were concluded by adding one-eighth volume of 30% (v/v) H_2O_2 and a 1:5 dilution with water. Metal content in digested samples was measured by furnace atomic absorption spectroscopy (Varian SpectrAA 880/GTA 100).

Enzymatic Assay of Superoxide Dismutase Activity—*M. smegmatis* strains were grown in Sauton's medium without the addition of metals or in the presence of 50 μM $MnCl_2$, $ZnSO_4$, $CoCl_2$, or $FeCl_2$, and secreted proteins were collected as indicated above. *M. tuberculosis* strains were grown in Sauton's medium, and secreted proteins were collected as stated above. Secreted fractions were resolved in 10% non-denaturing PAGE,

and gels were incubated for 30 min in 2.5 mM nitro blue tetrazolium (Sigma), followed by a 20-min incubation with 30 mM potassium phosphate, 30 mM TEMED, 30 mM riboflavin, pH 7.8 (43). Superoxide dismutase activity was visualized by illuminating gels with white light for 10 min on a transilluminator. Areas of activity were visible as white bands against a dark background. As a control, samples were run in independent gels and CBB-stained.

Liquid Chromatography Mass Spectroscopy—Supernatants obtained from *M. tuberculosis* and *M. smegmatis* wild type, *ctpC*::*hyg*, and complemented strain cultures were separated by 10% non-denaturing PAGE and CBB-stained. The corresponding bands from parallel gels showing superoxide dismutase activity were excised, destained by several dehydration-rehydration steps, and trypsin-digested for subsequent MS/MS analysis. Briefly, samples were dehydrated with acetonitrile and rehydrated in 100 mM NH_4HCO_3, 50% (v/v) acetonitrile. When most of the dye was removed, the samples were reduced with 10 mM DTT in 100 mM NH_4HCO_3, incubated for 35 min at 56 °C in a shaking incubator, and vacuum-dried. Alkylation was conducted by incubating for 30 min with 55 mM iodoacetamide in 100 mM NH_4HCO_3. After wash using 100 mM NH_4HCO_3, 50 μl of 100 mM NH_4HCO_3, 50% (v/v) acetonitrile were added to the pellet before the final drying step. The sample was digested by adding 30–50 μl of sequencing grade modified trypsin (Promega) and incubated overnight at 37 °C. Soluble peptides were extracted and combined with the result of three washes of 50 ml of 50% (v/v) acetonitrile, 5% (v/v) formic acid (15 min). Finally, digested samples were resolved in an Accurate-Mass Q-TOF LC/MS 6520, and peptide identification from collision-induced fragmentation patterns was performed with Spectrum Mill software (Agilent).

Mouse Infection—C57BL/6 female mice (8–10 weeks old) were infected with $\sim 1 \times 10^3$ CFU of wild type, *ctpC*::*hyg*, or *ctpC* complemented *M. tuberculosis* via the aerosol route. Groups of three mice were sacrificed at the indicated time points, and the bacterial burden in the lung homogenates was obtained by plating on 7H10 agar medium. In alternative competition experiments, two *M. tuberculosis* H37Rv strains (wild type and *ctpC*::*hyg* mutant or complemented) were mixed in a 3:1 ratio (6×10^5 CFU in a 200-μl final volume) and inoculated into the tail vein of female C57BL/6J mice. Groups of three mice were sacrificed at the indicated time points, and the bacterial burden in the lung homogenates was obtained by plating on 7H10 agar medium with or without 100 μg/ml hygromycin for mutant CFU and total CFU counting, respectively. Mice were housed under specific pathogen-free conditions and in accordance with University of Massachusetts Medical School Institutional Animal Care and Use Committee guidelines.

RESULTS

CtpC Is a Novel ATPase—CtpC belongs to the family of P_{1B}-ATPases. As such, it is characterized by the presence of eight TMs in a typical membrane topology, the cytoplasmic actuator, ATP binding, and phosphorylation domains (Fig. 1*A*) (19, 20). This last cytosolic loop contains the DKTGT sequence common to all P-type ATPases, where the conserved Asp is phosphorylated during catalysis. Considering the conservation of major catalytic domains and transmembrane overall structure, it is not surprising that the primary sequence of CtpC is similar (26–36% identity) to that of Cu^+-ATPases and Zn^{2+}ATPases, leading to a hypothesis suggesting Cu^+ and Zn^{2+} as likely substrates (11, 20). BLAST searches revealed the presence of proteins with structural characteristics similar to those of CtpC only in a few mycobacterial species, *Rhodococcus opacus*, *Kineococcus radiotolerans*, and *Nakamurella multipartite* (Fig. 1*B*). CtpC homologs lack the well described regulatory cytoplasmic N-MBDs that are ubiquitous in Cu^+- and Zn^{2+}-ATPases (20). More important, CtpC proteins present differences in metal-coordinating transmembrane residues. Invariant amino acids in TMs flanking the ATP binding domain are critical for the metal specificity of P_{1B}-ATPases because these coordinate the metal substrates during transport (19–23). Alignment of CtpC sequences corresponding to the sixth, seventh, and eighth TM segments showed the presence of two conserved Cys residues in TM6, Asn and Tyr in TM7, and His, Asn, and two Ser residues in TM8 (Fig. 1, *A* and *B*). Comparison with ligand donor amino acids in substrate binding sites of Cu^+-, Co^{2+}-, and particularly Zn^{2+}-ATPases shows significant differences, suggesting that CtpC might be involved in the transport of an alternative metal (Fig. 1*C*) (19–23).

CtpC Is a Unique Mn^{2+}-ATPase—To avoid the complexity of *in vivo* systems, the substrates of *M. tuberculosis* CtpC were biochemically characterized using purified protein. *M. tuberculosis ctpC* was cloned and expressed in *E. coli*. The resulting protein was solubilized and purified by metal affinity chromatography, and the engineered His_6 tag was removed by tobacco etch virus protease treatment (Fig. 2*A*). A functional preparation was obtained by reconstituting the protein in lipid/detergent micelles. The central characteristic of the transport mechanism of all P-ATPases is the coupling of transmembrane substrate transport to ATP hydrolysis (3, 19). Stimulation of ATP hydrolysis by substrates is a proven approach to evaluate the substrate specificity of these enzymes. *M. tuberculosis* CtpC ATPase activity was stimulated by the presence of various metals in the assay media (Fig. 2*B*). Under metal-saturating conditions, CtpC exhibited a maximum ATPase activity in the presence of Mn^{2+} and to a smaller extent (25–30%) by Co^{2+}, Cu^{2+}, and Zn^{2+}. It is equally significant that other metals, such as Cu^+, Ni^{2+}, Fe^{2+}, and Cd^{2+}, did not activate CtpC (Fig. 2*B*) because Zn^{2+}-ATPases are also activated by Cd^{2+} (44, 45), and a role in Fe^{2+} transport might be suggested by certain phenotypic observations (see below). Cleavage of the His_6 tag or the presence of thiols in the assay media had no effect on metal activation patterns (data not shown). Fig. 2*C* shows the dependence of CtpC ATPase activity on the Mn^{2+} and Zn^{2+} concentration. Interestingly, CtpC turnover (V_{max}) (Table 2) is remarkably slow when compared with enzymes involved in metal detoxification and tolerance, such as *E. coli* CopA (10-fold higher V_{max}) (46), *Pseudomonas aeruginosa* CopA1 (4-fold higher) (41), *E. coli* ZntA (10-fold higher) (44), or *Archaeoglobus fulgidus* CopA (4-fold higher) (33). In fact, CtpC V_{max} is more similar to *P. aeruginosa* CopA2, a slow transporting Cu^+-ATPase involved in cytochrome *c* oxidase assembly (41). The apparent high affinity of CtpC for Mn^{2+} is also consistent with this function. Although the estimation of relative metal affini-

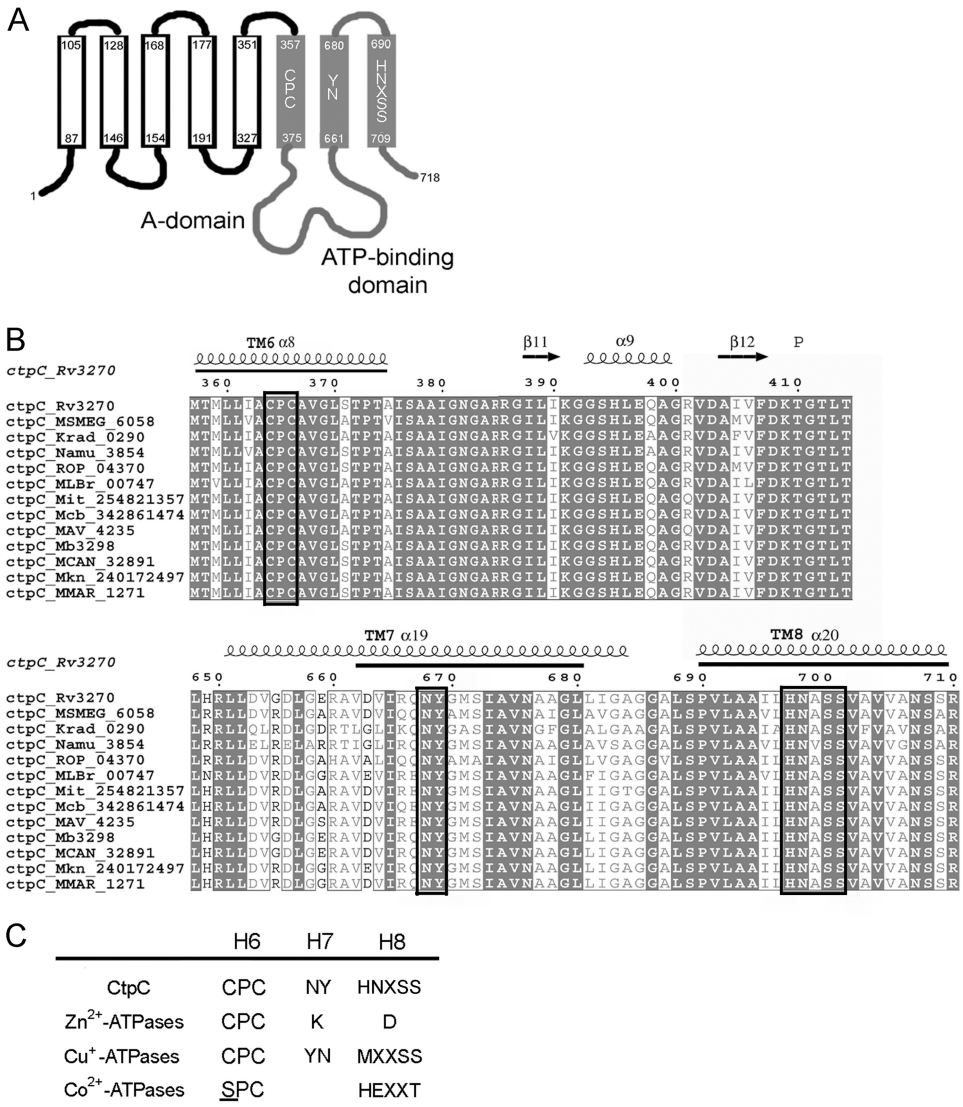

FIGURE 1. **CtpC structure.** *A*, membrane topology of *M. tuberculosis* CtpC and location of the conserved residues in TM6, TM7, and TM8 of CtpC. *B*, partial alignment of CtpC homologous protein sequences corresponding to TM6 and phosphorylation site DKTGT (*top*) and TM7 and TM8 (*bottom*). Sequences are from Rv3270, *M. tuberculosis*; MSMEG_6058, *M. smegmatis* strain $mc^{2}155$; Krad_0290, *Kineococcus radiotolerans* SRS30216; Namu_3854, *Nakamurella multipartite*; ROP_04370, *Rhodococcus opacus* B4; MLBr_00747, *Mycobacterium leprae* Br4923; Mit_254821357, *Mycobacterium intracellulare* ATCC 13950; Mcb_342861474, *Mycobacterium colombiense* CECT 3035; MAV_4235, *Mycobacterium avium* 104; Mb3298, *Mycobacterium bovis* AF2122/97; MCAN_32891, *Mycobacterium canettii*; Mkn_240172497, *Mycobacterium kansasii*; MMAR_1271, *Mycobacterium marinum*. Putative TM segments (*black bars*) and likely metal coordinating amino acids (*red rectangles*) are indicated. *C*, comparison of metal-coordinating residues of CtpC, Cu^{+}-, Zn^{2+}-, and Co^{2+}-ATPases.

ties requires equilibrium binding experiments and the low ATPase activity hampers precise activation $K_{½}$ determinations, it is clear that CtpC interacts with Mn^{2+} and Zn^{2+} with very high affinities (Table 2). The CtpC estimated $K_{½}$ value for activation is ~1–2 orders of magnitude lower than those seen in other P_{1B}-ATPases (33, 44, 46, 47). These observations were further confirmed by analysis of the homologous *M. smegmatis* CtpC. The heterologously expressed and purified *M. smegmatis* protein showed metal activation and biochemical parameters identical to those of the *M. tuberculosis* CtpC (Table 2).

Invariant amino acids located in TMs determine metal specificity and, as metal ligands, are required for enzyme function (19–23). Although a full analysis of metal coordination by CtpC is beyond this report, the importance of the distinct H*XX*SS sequence in TM8 of *M. tuberculosis* CtpC was explored. As expected, proteins carrying point mutant H699A and neighboring S700A/S701A showed no ATPase activity at saturating Mn^{2+} levels (Fig. 2*D*). This supports the link between the observed Mn^{2+}-dependent ATPase activity and the binding of this metal to a transmembrane transport site distinct from those in Cu^{+}- or Zn^{2+}-ATPases.

The observed biochemical properties, low transport rate, and high apparent metal affinity suggest that CtpC might perform a role other than detoxifying the cells by exporting cytoplasmic metals into the extracellular media (3, 41). However, the modest activation of CtpC by Zn^{2+} and the previously proposed role for this protein as a Zn^{2+}-ATPase controlling cytoplasmic levels of this metal (11) prompted us to confirm that this protein's specificity was not altered *in vivo*. To test this, we complemented a *zntA*::*kan* RW3110 *E. coli* strain, lacking the functional Zn^{2+}-ATPase (32), with *M. tuberculosis* CtpC. Fig. 3*A* shows that, although Zn^{2+} tolerance is restored by comple-

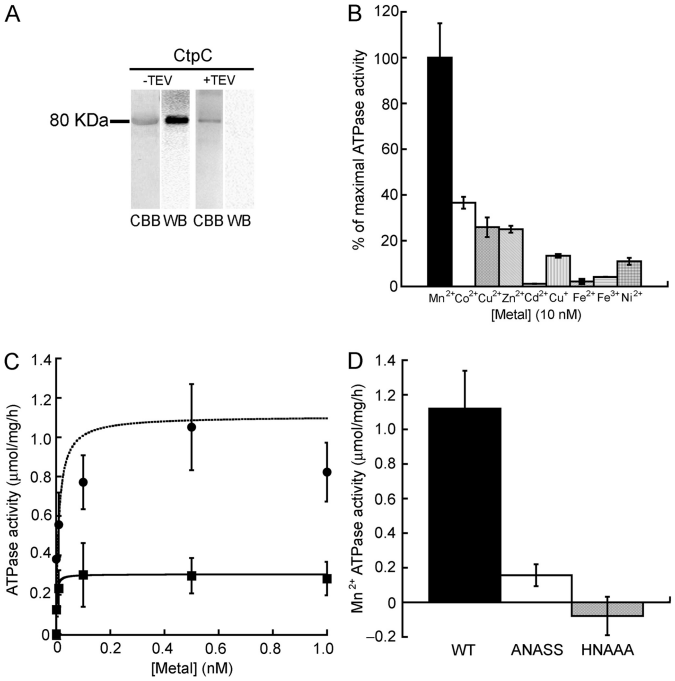

FIGURE 2. **Biochemical characterization of *M. tuberculosis* CtpC.** *A*, CtpC purification. 20 μg of CtpC, treated and untreated with tobacco etch virus protease, was resolved in SDS-PAGE and CBB-stained or immunostained (*WB*). *B*, CtpC ATPase activity in the presence of 10 nM metals (saturating concentration). 100% = 1.1 μmol/mg/h activity. *C*, CtpC ATPase activity dependence on Mn^{2+} (●) and Zn^{2+} (■). Curves were fit to the equation, $v = V_{max}\ L/(L + K_{1/2})$, where L is the concentration of variable ligand. Data obtained at 10 and 100 μM metal are not shown but were included in curve fitting. Fitting parameters are presented in Table 2. *D*, Mn^{2+}-ATPase activity of H697A and S700A/S701A CtpC mutants. In all experiments, data points represent the mean ± S.E. (*error bars*) of at least three independent experiments performed in duplicate.

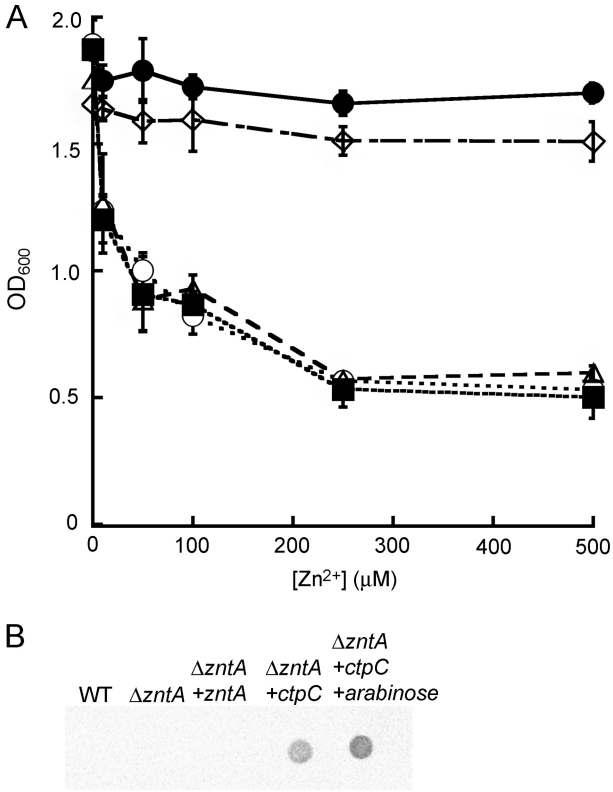

FIGURE 3. **Lack of functional complementation of Δ*zntA E. coli* by *ctpC*.** *A*, effect of Zn^{2+} on the growth of *E. coli* W3310 wild type (●), Δ*zntA* (○), Δ*zntA* complemented with *E. coli zntA* (◇), and *M. tuberculosis ctpC* transformed Δ*zntA* strains (■, uninduced; △, arabinose-induced). *B*, expression of CtpC in transformed Δ*zntA E. coli* cells. Dot blotted cells immunostained with anti-His_6 tag antibody. *Error bars*, S.E.

TABLE 2

Free metal ATPase activity kinetic parameters of *M. tuberculosis* and *M. smegmatis* CtpC

Metal	*M. tuberculosis* CtpC		*M. smegmatis* CtpC	
	V_{max}	$K_{1/2}$	V_{max}	$K_{1/2}$
	μmol/mg/h	nM	μmol/mg/h	nM
Mn^{2+}	1.1 ± 0.2[a]	0.009 ± 0.008	1.06 ± 0.06	0.005 ± 0.002
Zn^{2+}	0.30 ± 0.01	0.019 ± 0.001	0.38 ± 0.07	0.02 ± 0.01

[a] Errors for V_{max} and $K_{1/2}$ are asymptotic S.E. values reported by the fitting software Kaleidagraph (Synergy).

menting *E. coli* with ZntA, *M. tuberculosis* CtpC introduced in a similar construct was unable to rescue the *E. coli zntA* mutant when grown in the presence of high Zn^{2+} levels. Fig. 3*B* shows the expression of CtpC under the tested conditions. These results indicate that CtpC is unlikely to play a role in controlling cytoplasmic Zn^{2+} levels.

CtpC Deficiency Renders M. tuberculosis Sensitive to Zn^{2+} and Oxidative Stress—It has been reported that deletion of *ctpC* decreases the Zn^{2+} tolerance of the *M. tuberculosis* GC1257 strain (11). We observed a similar phenotype in *M. tuberculosis* H37Rv *ctpC*::*hyg* cells when grown at Zn^{2+} concentrations as low as 5 μM (Fig. 4*A*). However, no changes were observed in the sensitivity to Cd^{2+}, a metal that usually shows similar toxicity in Zn^{2+} mutants or to the enzyme substrate Mn^{2+} (Fig. 4, *B* and *C*). Similarly, the presence of Co^{2+} or Cu^{2+} in the medium had no effect on the growth of these cells (data not shown). Reasoning that Zn^{2+} could impose oxidative stress, we determined if the *ctpC* mutant was sensitive to other oxidants. Indeed, we found that this mutant was hypersensitive to both *tert*-butyl hydroperoxide (*TBHP*; Fig. 4*D*) and superoxide (generated with hypoxanthine/xanthine oxidase; Fig. 4*E*). In both cases, the wild type phenotype was restored in the complemented strain. Correlating with the alterations in Zn^{2+} tolerance, a significant induction of *ctpC* expression in response to Zn^{2+} was detected (Fig. 4*F*) (11). This induction was not observed when cells were challenged with other tested stressors (Fig. 4*F*). These data imply a complex system in which *ctpC* expression is neither induced by nor confers resistance to its substrate Mn^{2+}. However, the enzyme is required for tolerance to Zn^{2+} and oxidative stress. To explain these observations, the role of CtpC in *M. smegmatis* was studied. Surprisingly, the *M. smegmatis ctpC*::*hyg* strain showed no higher sensitivity to Zn^{2+} (Fig. 5*A*), although it behaved as the *M. tuberculosis* mutant in the presence of Mn^{2+} (no effect; Fig. 5*B*) and redox stress (increased sensitivity; Fig. 5*C*). Furthermore, contrary to the observation that Zn^{2+} stimulates *M. tuberculosis ctpC* expression, no induction was observed in *M. smegmatis* when exposed to the metal (Fig. 5*D*). Interestingly, a 15-fold increase in *ctpC* expression was observed when *M. smegmatis* was exposed to the extracellular superoxide generator hypoxanthine/xanthine oxidase.

Deletion of ctpC Leads to Cytoplasmic Mn^{2+} Accumulation and a Decrease in Secreted Mn^{2+}-bound Proteins—Based on the role of well described P_{1B}-ATPases in controlling cellular

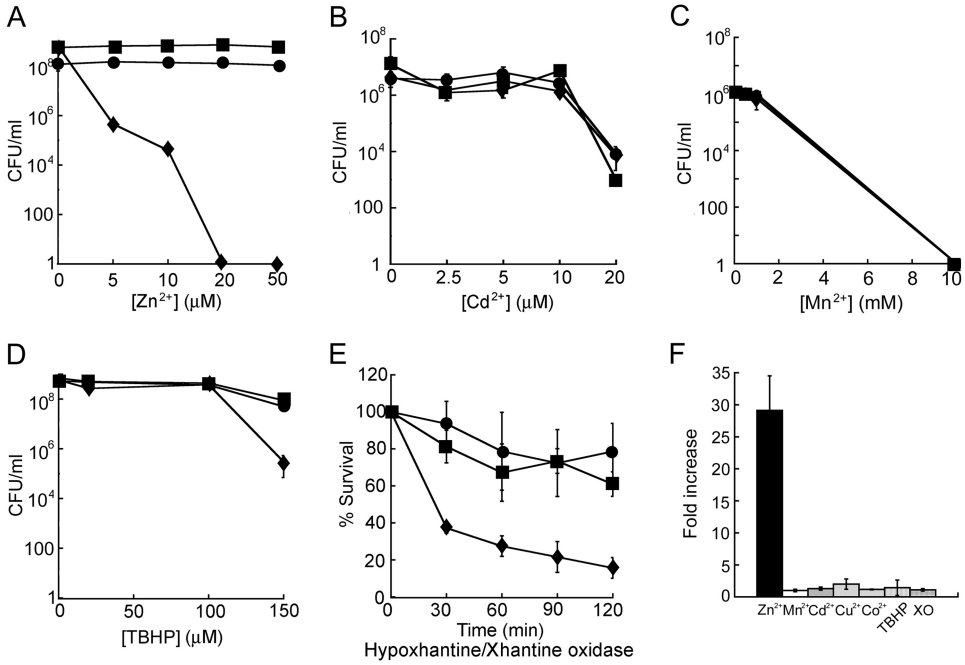

FIGURE 4. **Response of *M. tuberculosis ctpC*::*hyg* strain to metal and redox stressors.** *A–D*, *M. tuberculosis* H37Rv wild type (●), *ctpC*::*hyg* (♦), and complemented (■) strains were grown in the presence of increasing concentrations of the indicated stressor and plated on 7H10 agar plates, and CFU were counted and normalized by ml of culture. *E*, *in vitro* susceptibility of *M. tuberculosis* H37Rv wild type (●), *ctpC*::*hyg* (♦) and complemented (■) strains to extracellular redox stress. Cells were treated with 250 mM hypoxanthine and 0.1 unit/ml xanthine oxidase and plated on 7H10 agar plates at different time points. *F*, induction of *ctpC* expression in *M. tuberculosis* H37Rv cells incubated for 2 h with 100 μM $CuSO_4$, $ZnSO_4$, $CoCl_2$, $MnCl_2$, *tert*-butyl hydroperoxide (*TBHP*), and $FeCl_2$ or for 1 h with 250 mM hypoxanthine and 0.1 unit/ml xanthine oxidase. Samples were processed for qPCR analysis and normalized against *sigA*. Data are the mean ± S.E. (*error bars*) of three independent experiments.

metal quotas, the content of various transition metals in *ctpC* mutant *M. tuberculosis* cells was measured (Table 3). Under basal conditions, no changes in transition metal levels were observed except for a modest but significant increase of Mn^{2+} content. Considering the described Zn^{2+} accumulation in *M. tuberculosis* GC1237 *ctpC* mutant cells (11), Zn^{2+} levels under similar Zn^{2+} stress conditions were also analyzed. No Zn^{2+} accumulation was detected in our system (Tables 3 and 5). Mn^{2+} homeostasis was further analyzed in cells grown in the presence of 50 μM Mn^{2+}. Taking into account the proposed function of P_{1B}-ATPases on the metallation of periplasmic/secreted proteins, Mn^{2+} bound to periplasmic/secreted protein fractions was measured. To avoid interference from the presence of albumin in 7H9 medium, these experiments were performed in the more defined Sauton's medium. A 4-fold increase in cellular Mn^{2+} content was observed in the *M. tuberculosis ctpC* mutant, along with a significant decrease in the Mn^{2+} bound to secreted proteins (Fig. 6*A* and Table 4). On the contrary, the levels of Zn^{2+}, Fe^{2+}, or Cu^{2+} bound to secreted proteins were not affected in the *M. tuberculosis* or *M. smegmatis ctpC* mutant strain (Tables 4 and 5). *M. smegmatis ctpC* mutant cells allowed further analysis of subcellular fractions (Fig. 6*B*). A large increase of Mn^{2+} bound to cytosolic proteins was observed, along with a significant decrease in Mn^{2+} bound to secreted proteins. These results confirmed the function of CtpC as a Mn^{2+}-ATPase involved not only in maintaining cytoplasmic metal quotes but probably participating in the metallation of secreted Mn^{2+} proteins. Moreover, these observations suggest that CtpC might not be involved in conferring Zn^{2+} tolerance but rather in an alternative process, such as the response to redox stress. In the case of *M. tuberculosis, this* response to redox stress might be triggered by high Zn^{2+} levels.

CtpC Is Required for Functional Secreted SodA—The metallation of secreted Mn^{2+}-bound proteins appeared to be deficient in *ctpC* mutants, and some of these may be required for overcoming redox stress. Mn-SodA was a logical candidate for CtpC-mediated metallation. In mycobacteria, the SodA protein is secreted in the apo-form via the Sec pathway (18). Consequently, SodA probably acquires its metal in the extracellular milieu. The metal specificity of SodA-like enzymes is not predictable based on primary protein sequence. Although *M. tuberculosis* SodA appears to contain Fe^{2+}, other highly homologous SodAs are Mn^{2+} enzymes (17, 48, 49). Moreover, cambialistic properties have been observed in these enzymes, suggesting that distinct metals might be used by the same enzyme under different conditions. To test the putative role of CtpC in the metallation of secreted SodA, in-gel superoxide dismutase activity assays were performed. The secreted fraction from *M. tuberculosis ctpC*::*hyg* strain showed a 37% decrease in the activity of SodA compared with wild type (Fig. 7, *A* and *B*). The SodA activity was partially recovered in the CtpC complement strain when compared with wild type, probably reflecting the levels of CtpC expression in the complemented cells. Interestingly, when analyzing the secreted SodA from *M. smegmatis ctpC*::*hyg* mutant, the activity decreased up to 80% compared with the SodA obtained from the wild type strain (Fig. 7, *C* and *D*). CBB staining of identical gels showed no decrease SodA protein secretion (Fig. 7*C*, *bottom*). The identity of secreted SodA was verified by liquid chromatography/mass spectrometry (LC/MS; Table 6). Because mycobacteria also

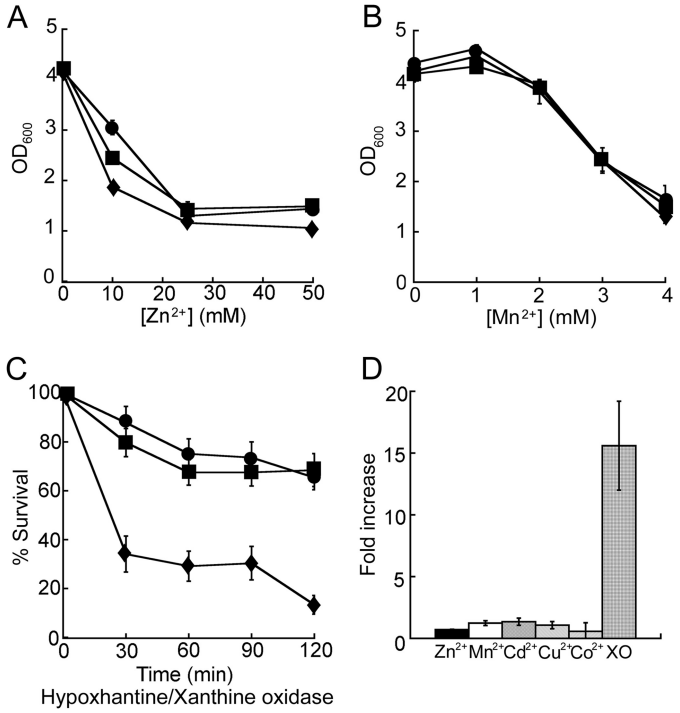

FIGURE 5. **Response of *M. smegmatis ctpC::hyg* to metal and redox stressors.** *M. smegmatis* wild type (●), *ctpC::hyg* (♦), and complemented (■) strains were grown in 7H9 medium supplemented with increasing concentrations of Zn^{2+} (*A*) or Mn^{2+} (*B*) for 48 h, and A_{600} was determined. *C*, *in vitro* susceptibility of *M. smegmatis* wild type (●), *ctpC::hyg* (♦), and complemented (■) strains to extracellular redox stress. Cells were treated with 250 mM hypoxanthine and 0.1 unit/ml xanthine oxidase and plated on 7H10 agar plates at different time points. *D*, induction of *ctpC* expression in *M. smegmatis* wild type cells incubated for 2 h with 100 μM $CuSO_4$, $ZnSO_4$, $CoCl_2$, $MnCl_2$, *tert*-butyl hydroperoxide, and $FeCl_2$ or for 1 h with 250 mM hypoxanthine and 0.1 unit/ml xanthine oxidase. Samples were processed for qPCR analysis and normalized against *sigA*. Data are the mean ± S.E. (*error bars*) of three independent experiments.

TABLE 3

***M. tuberculosis ctpC::hyg* mutant accumulates Mn^{2+}**

Metal[a]	Whole cell metal content		
	Wild type	*ctpC::hyg*	Complemented
	pmol/mg protein		
7H9 medium			
Manganese	1.2 ± 0.3	2.1 ± 0.1[b]	1.7 ± 0.1
Zinc	317 ± 12	283 ± 5	314 ± 23
Copper	28 ± 6	25 ± 1	28 ± 3
Cobalt	0.31 ± 0.04	0.23 ± 0.02	0.26 ± 0.06
Iron	237 ± 38	192 ± 7	455 ± 13
7H9 medium + Zn^{2+}			
Zinc	654 ± 18	581 ± 35	689 ± 28

[a] Cells were grown to log phase.
[b] Statistical significance at $p < 0.037$.

have cytoplasmic Cu/Zn-SodCs, it is also relevant that no differences were found when analyzing total superoxide dismutase activity in whole cell homogenates or cytosolic or membrane fractions obtained from *M. smegmatis* wild type, *ctpC::hyg*, and the complemented strains (data not shown).

Because of the mentioned cambialistic properties of SodA (50–52), we determined if *M. smegmatis* SodA activity could be restored by other metal co-factors independently of CtpC activity. *M. smegmatis* wild type, *ctpC::hyg*, and the complemented strains were grown in Sauton's medium supplemented with 50 μM $MnCl_2$, $FeCl_2$, $ZnSO_4$, or $CoCl_2$ until late log phase. In-gel

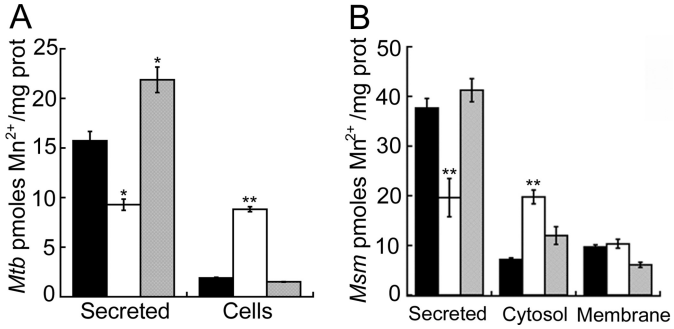

FIGURE 6. **Effect of *ctpC* deletion on protein-bound Mn^{2+} homeostasis.** *M. tuberculosis* (*A*) and *M. smegmatis* (*B*) wild type (*black bars*), *ctpC::hyg* (*white bars*), and complemented (*gray bars*) strains were grown in the presence of 50 μM Mn^{2+}. The protein-bound Mn^{2+} content in different cellular fractions was determined by furnace atomic absorption spectroscopy. Significant differences from the wild type as determined by Student's *t* test are indicated. *, $p \leq 0.008$; **, $p \leq 0.002$. *Error bars*, S.E.

TABLE 4

Secreted fraction metal content of *M. tuberculosis* strains

Metal[a]	Secreted fraction metal content		
	Wild type	*ctpC::hyg*	Complemented
	pmol/mg protein		
Manganese	15.7 ± 0.9	9.2 ± 0.5	22 ± 1
Zinc	105 ± 2	91 ± 21	99 ± 2
Copper	38 ± 10	36 ± 10	30 ± 7
Iron	605 ± 8	583 ± 20	613 ± 12

[a] Cells were cultured on Sauton's medium supplemented with 50 μM Mn^{2+}.

superoxide dismutase activity assays showed that SodA activity was restored when adding $MnCl_2$ or $FeCl_2$ to the culture medium of the *M. smegmatis ctpC::hyg* mutant strain (Fig. 7*C*). The addition of $ZnSO_4$ and $CoCl_2$ had no effect on this activity. No differences were observed in the activity of the secreted SodA from the wild type and complemented strains (data not shown). These data further support an important role for CtpC in the Mn^{2+} metallation of mycobacterial SodA during metal starvation stress. Fe^{2+} metallation appears to be unaffected, and under certain culture conditions, this prosthetic group may be used (17). The alternative use of these metal cofactors by SodA is addressed under "Discussion."

Considering the requirement of CtpC for Mn^{2+} secretion and SodA metallation and the lack of *ctpC* induction under Mn^{2+} excess (Figs. 4*F* and 5*D*), it is tempting to hypothesize that under Mn^{2+} starvation, *ctpC* expression should be induced. Although all of the media used in these studies have no Mn^{2+} formally included, interestingly, a 3.0 ± 0.3- and a 2.12 ± 0.06-fold increase in *ctpC* expression was observed when *M. smegmatis* cells were cultured in chelexed (0.3 nM Mn^{2+}) and non-chelexed (0.4 nM Mn^{2+}) Sauton's media, respectively, compared with those maintained in 7H9 medium (0.9 nM Mn^{2+}). Although small changes in Mn^{2+} levels might affect *ctpC* transcription, these are very small and unlikely to be of physiological significance.

CtpC Is Important for M. tuberculosis Virulence—Large scale genetic studies have predicted that *ctpC* is required for the growth or survival of *M. tuberculosis* H37Rv in the C57BL/6 mouse model of tuberculosis (24). More recent studies have reported that mutation of the *ctpC* gene impairs the intracellular growth of *M. tuberculosis* strain GC1237 in human macrophages but does not alter the virulence of this strain in BALB/C

TABLE 5
***M. smegmatis* cytosolic and secreted fraction metal levels**

Metal[a]	Cytosolic fraction			Secreted fraction		
	Wild type	*ctpC::hyg*	Complemented	Wild type	*ctpC::hyg*	Complemented
	pmol/mg protein			*pmol/mg protein*		
Manganese	7.1 ± 0.9	20 ± 1	12 ± 2	38 ± 3	20 ± 4	41 ± 2
Zinc	596 ± 17	519 ± 47	492 ± 67	182 ± 13	162 ± 24	168 ± 34
Copper	8 ± 2	4 ± 1	9 ± 3	22 ± 4	14 ± 2	27 ± 3
Iron	489 ± 24	457 ± 59	480 ± 43	629 ± 36	784 ± 45	617 ± 28

[a] Cells were cultured on Sauton's medium supplemented with 50 μM Mn^{2+}.

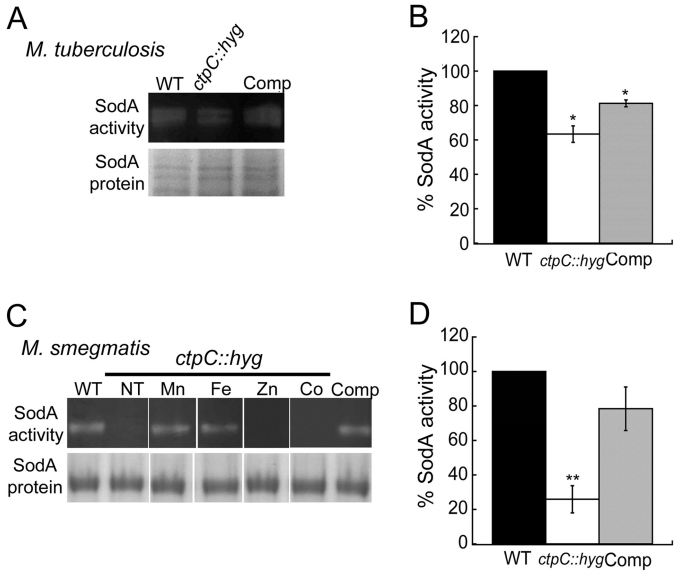

FIGURE 7. **Effect of *ctpC* deletion on the activity of secreted SodA.** *A*, in-gel SodA activity following separation of *M. tuberculosis* secreted protein fraction in non-denaturing PAGE (*top*). Similar gels were CBB-stained to visualize protein levels (*bottom*). *B*, densitometry of *M. tuberculosis* SodA activity bands. *C*, in-gel SodA activity following separation of *M. smegmatis* secreted protein fraction in non-denaturing PAGE (*top*). Similar gels were CBB-stained to visualize protein levels (*bottom*). The mutant *ctpC::hyg* strain was grown in a 50 μM concentration of the indicated metals. *NT*, non treated; *Comp*, complemented. *D*, densitometry of *M. smegmatis* SodA activity bands. Data are the mean ± S.E. (*error bars*) of at least three independent experiments. Significant differences from the wild type as determined by Student's *t* test are indicated. *, $p \leq 0.002$; **, $p \leq 0.001$.

or SCID mice (11). To verify the importance of CtpC for *M. tuberculosis* virulence, we assessed the growth of the *ctpC*::*hyg* mutant strain in two different models of tuberculosis. First, *M. tuberculosis* H37Rv, *ctpC*::*hyg*, and *ctpC* complemented strains were used to infect the relatively resistant C57BL/6 mouse strain via the low dose aerosol route. The *ctpC*::*hyg* strain grew similarly to wild type *M. tuberculosis* during the initial phase of infection that is governed by innate immune mechanisms. However, a significant decrease in viable *ctpC*::*hyg* bacteria was noted after a month of infection (Fig. 8*A*). This specific persistence defect is similar to that of mutants that are unable to resist the adaptive immune response (53). The attenuation of this mutant was confirmed using a more sensitive competitive model in which the ratio of mutant *versus* wild type bacteria was monitored in animals that were co-infected via the intravenous route. As we observed in the single-strain infections, the *ctpC*::*hyg* mutant was significantly underrepresented after 42 days of infection (Fig. 8*B*). The attenuation of this strain was observed at earlier time points in the competitive model (21 days), probably due to the earlier onset of adaptive immunity after intravenous challenge (54). No differences in growth were observed between wild type and complemented strains *in vitro* (not shown), and genetic complementation reversed the *in vivo* growth/survival defects of this mutant. Thus, *ctpC* is required for the bacterium to adapt to the host environment and appears to be specifically important for resisting the adaptive immune response.

DISCUSSION

Large scale genetic screens implicated *ctpC* in the adaptation of *M. tuberculosis* to the host environment (24). Recent studies have shown that an *M. tuberculosis ctpC* mutant is sensitive to Zn^{2+} (11), a metal that appears to accumulate in the phagosome (9). Taking into account these phenotypes and CtpC homology with Cu^{+}- and Zn^{2+}-ATPases, it was proposed that CtpC was a Zn^{2+}-ATPase involved in the efflux of cytoplasmic Zn^{2+} (11). However, CtpC lacks signature residues that are part of the transmembrane metal binding sites of Cu^{+}- and Zn^{2+}-ATPases, suggesting that it might transport alternative metals. Considering its putative importance for virulence and unique structure, the function of CtpC in *M. tuberculosis* and *M. smegmatis* was examined using a combination of biochemical and genetic approaches. Here, we describe that CtpC shows a preference for Mn^{2+}, controls the Mn^{2+} cytoplasmic quota, and is involved in the uploading of Mn^{2+} into secreted metalloproteins. We propose that these activities of CtpC are important for *M. tuberculosis* virulence.

CtpC is a metal transport P_{1B}-ATPase with characteristic phosphorylation domains and membrane topology, although it lacks the regulatory N-MBDs ubiquitous in enzymes with specificity for Cu^{+} or Zn^{2+} (19, 20). It is now well established that metal specificity is conferred by conserved residues in the TMs flanking the large cytoplasmic ATP binding and hydrolysis domain (19–23). Consequently, despite the significant similarity between CtpC and Cu^{+}/Zn^{2+}-ATPases, it lacks the sets of invariant metal-coordinating residues found in well characterized P_{1B}-ATPases, particularly the Lys and Asp in TM7 and TM8 that characterize Zn^{2+}-ATPases (20, 22). The analysis of the 13 sequences of homologous CtpC proteins showed that although these have retained the CPC signature in TM4, they have a unique NY in TM7 and HNASS in TM8. The presence of these unique residues is not trivial because their replacement leads to inactive proteins. It is interesting that although these residues resemble the Cu^{+} binding sequences (19–21), the replacement of Met for His (a harder Lewis base) is consistent with selectivity for Mn^{2+} (a hard Lewis acid), the substrate of CtpC identified in our studies. Moreover, the Ser (a hard Lewis base) conserved in CtpC provides further specificity toward Mn^{2+}. This Ser is absent in Zn^{2+} sites (55, 56).

TABLE 6
Peptides identified by LC/MS corresponding to superoxide dismutase from *M. tuberculosis and M. smegmatis*

Strain	Identified peptides	Protein	Accession number
M. tuberculosis wild type	AFWNVVNWADVQSREDHSAILLNEKYAATSQTKNL SPNGGDKPTGELAAAIADAFGSFDKAKEDHSAILLNEK	SodA superoxide dismutase (iron). *M. tuberculosis* H37Rv	NP_218363
M. tuberculosis ctpC::*hyg*	AFWNVVNWADVQSRYAATSQTKAKEDHSAILLNEKEDH SAILLNEK	SodA superoxide dismutase (iron). *M. tuberculosis* H37Rv	NP_218363
M. smegmatis wild type	AFWNVVNWDDVQNRNKSPNGGDKPTGELAAAIDDQFG SFDK	Msmeg_6427 superoxide dismutase (manganese)	ABK71950
M. smegmatis ctpC::*hyg*	AFWNVVNWDDVQNR	Msmeg_6427 superoxide dismutase [Mn]	ABK71950

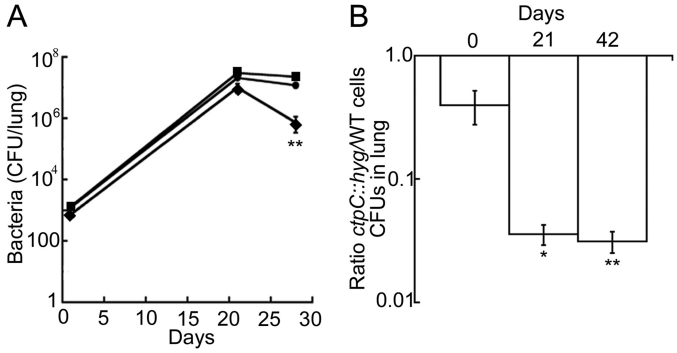

FIGURE 8. **CtpC is required for *M. tuberculosis* virulence.** *A*, *M. tuberculosis* H37Rv growth fitness of wild type (●), *ctpC*::*hyg* (♦), and complemented (■) strains after 21 and 28 days of infection. *B*, relative *in vivo* growth rates of wild type and *ctpC*::*hyg M. tuberculosis* H37Rv strains after 21 and 42 days of mouse infection. Means ± S.E. from 3–5 mice are shown. Significant differences from the wild type as determined by Student's *t* test are indicated. *, $p < 0.015$; **, $p < 0.01$. *Error bars*, S.E.

Direct biochemical analysis of CtpC activity showed that maximum activation of the transporter occurs in the presence of Mn^{2+}. However, Zn^{2+}, Co^{2+}, and even Cu^{2+} can act as alternative substrates although at slower turnover rates. This is not surprising because many Zn^{2+}-ATPases and Cu^{+}-ATPases can transport alternative metals sharing similar chemical properties (33, 44, 47, 57). Furthermore, it is significant that CtpC is not activated by Cd^{2+}, a well characterized activator of Zn^{2+}-ATPases (44, 58). However, it is perhaps more important to consider the high apparent affinity of CtpC for Mn^{2+} and that its activity is relatively slow compared with that of enzymes responsible for maintaining cytoplasmic metal quotas. If the reported activity of *E. coli* Zn^{2+}-ATPase is considered, the Zn^{2+}-ATPase activity of CtpC is 2 orders of magnitude lower when measured under practically identical conditions. This kinetic difference probably explains the inability of CtpC to confer Zn^{2+} tolerance and functionally complement a Δ*zntA E. coli* mutant. We hypothesize that in *M. tuberculosis*, the necessary Zn^{2+} efflux is mediated by the cation diffusion facilitator coded by *Rv2025*. This is homologous to the *M. smegmatis* Zn^{2+} transporter ZitA (59) and *E. coli* ZitB (60).

Whereas biochemical determinations provide a direct evaluation of heavy metal transport ATPase substrates, characterization of cellular roles might provide further insight into the enzyme selectivity. Determination of metal contents and tolerance to metal stress as well as induction of gene expression by putative substrates are commonly used indicators of substrate specificity. We observed little or no sensitivity of the *ctpC*::*hyg* cells to various metal stressors, except for the described lack of tolerance to Zn^{2+} (11). This phenotype was not observed in *M. smegmatis*, suggesting that *M. tuberculosis* is particularly sensitive to Zn^{2+} or to an associated stress (see below). Interestingly, the lack of Zn^{2+} tolerance was correlated with a lack of induction of the *ctpC* gene by Zn^{2+} in *M. tuberculosis*. On the other hand, it was also remarkable that the Cd^{2+} did not induce *ctpC* expression, suggesting that *ctpC* expression is not driven by Zn^{2+}-sensing transcriptional regulators (61).

We observed that mutation of *ctpC* led to an increase in intracellular Mn^{2+} levels but did not affect the cellular Zn^{2+}, Co^{2+}, or Fe^{2+} content. Mn^{2+} is apparently nontoxic to the cells because high (millimolar) extracellular Mn^{2+} is necessary to affect cell growth. Noticeably, the Mn^{2+} accumulation was observed even in basal medium conditions; it was more prominent in cells grown in 50 μM Mn^{2+}. These findings are consistent with our biochemical data, although we did not observe the previously described Zn^{2+} accumulation in *ctpC* mutant cells under Zn^{2+} stress conditions (11). These differences might be associated with alternative Zn^{2+} efflux systems present in the different strains of *M. tuberculosis* used in these experiments. Previous work employed the *M. tuberculosis* GC1237 strain, whereas we characterized the *ctpC*::*hyg* mutant in the H37Rv background. Still, our *in vivo* observations support the conclusion that this CtpC functions primarily as a Mn^{2+} transporter.

Given this biochemical function, the Zn^{2+} sensitivity and the Zn^{2+}-dependent *ctpC* expression observed in *M. tuberculosis* are unexpected. It might be considered that metal homeostasis is linked to other cellular phenomena (*e.g.* the redox equilibrium). In particular, the association of Zn^{2+}, Mn^{2+}, and Fe^{2+} transporters in several redox-responsive regulons has been documented (62, 63). Expression of the *ctpC* gene is induced in low Fe^{2+} conditions (27), and it is possible that high Zn^{2+} concentrations might mimic Fe^{2+} deficiency. Alternatively, a link between Zn^{2+} and σ factors has been proposed in *M. tuberculosis* (64), and reactive oxygen species have been shown to affect the signaling pathways involved in the activation of multiple transcription factors (65). Considering the observation that *ctpC*::*hyg* cells are also sensitive to redox stressors, it is tempting to speculate that the sensitivity to Zn^{2+} is related to alteration in Fe^{2+} or redox homeostasis rather than to an increase in cytosolic Zn^{2+}. The increased susceptibility of both mycobacterial *ctpC*::*hyg* mutants to the oxidative stress produced by xanthine oxidase supports these ideas.

An alternative link between Zn^{2+} and redox stress might also be considered. In *M. tuberculosis*, metallothioneins are primary barriers against Cu^{+} toxicity (66). There is evidence that these proteins also bind Zn^{2+} and Cd^{2+} with high affinity. Both ions could generate an imbalance in cell redox through mechanisms such as mycothiol consumption, thioredoxins inhibition, or Cu^{+} displacement by competition when present at high con-

centrations (67). The addition of Zn^{2+} to the media might release Cu^{+} from oxidized metallothioneins, the former generating reactive oxygen species by means of the Fenton reaction. Contrary to Zn^{2+}, 50 μM Cd^{2+} induces the transcription of metallothioneins in *M. tuberculosis* (66). The induction of metallothioneins by Cd^{2+} might explain why *M. tuberculosis ctpC* is not sensitive to Cd^{2+} when compared with the wild type strain H37Rv.

CtpC is required for *M. tuberculosis* growth and survival in the mouse model. The importance of Mn^{2+} for the virulence of other bacterial pathogens has been described, although Mn^{2+} levels in the phagosome might not change dramatically during infection (9, 49). Our biochemical and phenotypic analyses indicate that CtpC, although it partially influences cytoplasmic Mn^{2+} levels, is a slow ATPase, its expression is not induced by its substrate, and CtpC-deficient cells exhibit normal tolerance to Mn^{2+} metal excess. These are all characteristics similar to those observed in Cu^{+}-ATPases responsible for assembly of cytochrome *c* oxidase instead of cytosolic detoxification (41). In agreement with this putative role, the *ctpC*::*hyg* mutant showed a decrease in the amount Mn^{2+}-bound to secreted proteins. Further experiments showed that deletion of *ctpC* reduced secreted Mn^{2+}/Fe^{2+}-SodA activity without altering the abundance of the protein, suggesting that the enzyme might not be metallated. Supporting this hypothesis, *M. smegmatis* SodA activity was restored by supplementing the growth medium with either Mn^{2+} or Fe^{2+}. Secreted metalloproteins, such as SodA, have been shown to be required for virulence (14, 16). Both *M. tuberculosis* and *M. smegmatis* SodA are highly homologous and lack a classical signal sequence for protein export (68), although *M. tuberculosis* SodA is exported via the SecA2 pathway, which exports unfolded apoproteins (18). Interestingly, one important difference between them is the metal co-factor either SodA acquires *in vitro*. *M. tuberculosis* SodA has been characterized as an Fe-superoxide dismutase, whereas *M. smegmatis* SodA contains Mn^{2+} (17). However, *M. smegmatis* SodA has a cambialistic behavior *in vitro*, being activated by Fe^{2+} when the pH is acidic (48). These enzymes differ in one of the metal-coordinating residues; *M. tuberculosis* contains a His instead of a Gln at position 145, which is present in *M. smegmatis* Mn^{2+}-SodA. However, replacing His-145 with Gln does not affect the metal binding in *M. tuberculosis*, as determined by x-ray crystallography (17). The specificity for iron of the tuberculosis SodA seems to be counterintuitive, considering that upon macrophage infection, *M. tuberculosis* cells must face and overcome iron starvation (8). Thus, it is possible that *M. tuberculosis* SodA is preferentially loaded with Mn^{2+} in the iron-limited *in vivo* environment.

In summary, the data presented indicate that CtpC is a unique Mn^{2+}-ATPase predominantly present in mycobacteria. The enzyme appears to be required for loading Mn^{2+} into secreted metalloproteins. In this role, the CtpC is a key element for virulence.

Acknowledgments—We thank Courtney McCann, K. G. Papavinasasundaram, and Xavier Meniche for valuable technical assistance.

REFERENCES

1. Macomber, L., and Imlay, J. A. (2009) The iron-sulfur clusters of dehydratases are primary intracellular targets of copper toxicity. *Proc. Natl. Acad. Sci. U.S.A.* **106,** 8344–8349
2. Valko, M., Morris, H., and Cronin, M. T. (2005) Metals, toxicity and oxidative stress. *Curr. Med. Chem.* **12,** 1161–1208
3. Argüello, J. M., González-Guerrero, M., and Raimunda, D. (2011) Bacterial transition metal P_{1B}-ATPases. Transport mechanism and roles in virulence. *Biochemistry* **50,** 9940–9949
4. Waldron, K. J., and Robinson, N. J. (2009) How do bacterial cells ensure that metalloproteins get the correct metal?. *Nat. Rev. Microbiol.* **7,** 25–35
5. Waldron, K. J., Rutherford, J. C., Ford, D., and Robinson, N. J. (2009) Metalloproteins and metal sensing. *Nature* **460,** 823–830
6. Osman, D., and Cavet, J. S. (2011) Metal sensing in *Salmonella*. Implications for pathogenesis. *Adv. Microb. Physiol.* **58,** 175–232
7. Forbes, J. R., and Gros, P. (2001) Divalent-metal transport by NRAMP proteins at the interface of host-pathogen interactions. *Trends Microbiol.* **9,** 397–403
8. Kehl-Fie, T. E., and Skaar, E. P. (2010) Nutritional immunity beyond iron. A role for manganese and zinc. *Curr. Opin. Chem. Biol.* **14,** 218–224
9. Wagner, D., Maser, J., Lai, B., Cai, Z., Barry, C. E., 3rd, Höner Zu Bentrup, K., Russell, D. G., and Bermudez, L. E. (2005) Elemental analysis of *Mycobacterium avium*-, *Mycobacterium tuberculosis*-, and *Mycobacterium smegmatis*-containing phagosomes indicates pathogen-induced microenvironments within the host cell's endosomal system. *J. Immunol.* **174,** 1491–1500
10. White, C., Lee, J., Kambe, T., Fritsche, K., and Petris, M. J. (2009) A role for the ATP7A copper-transporting ATPase in macrophage bactericidal activity. *J. Biol. Chem.* **284,** 33949–33956
11. Botella, H., Peyron, P., Levillain, F., Poincloux, R., Poquet, Y., Brandli, I., Wang, C., Tailleux, L., Tilleul, S., Charriere, G. M., Waddell, S. J., Foti, M., Lugo-Villarino, G., Gao, Q., Maridonneau-Parini, I., Butcher, P. D., Castagnoli, P. R., Gicquel, B., de Chastellièr, C., and Neyrolles, O. (2011) Mycobacterial P_1-type ATPases mediate resistance to zinc poisoning in human macrophages. *Cell Host Microbe* **10,** 248–259
12. Aydemir, T. B., Liuzzi, J. P., McClellan, S., and Cousins, R. J. (2009) Zinc transporter ZIP8 (SLC39A8) and zinc influence IFN-γ expression in activated human T cells. *J. Leukocyte Biol.* **86,** 337–348
13. Begum, N. A., Kobayashi, M., Moriwaki, Y., Matsumoto, M., Toyoshima, K., and Seya, T. (2002) *Mycobacterium bovis* BCG cell wall and lipopolysaccharide induce a novel gene, *BIGM103*, encoding a 7-TM protein. Identification of a new protein family having Zn-transporter and Zn-metalloprotease signatures. *Genomics* **80,** 630–645
14. Edwards, K. M., Cynamon, M. H., Voladri, R. K., Hager, C. C., DeStefano, M. S., Tham, K. T., Lakey, D. L., Bochan, M. R., and Kernodle, D. S. (2001) Iron-cofactored superoxide dismutase inhibits host responses to *Mycobacterium tuberculosis*. *Am. J. Respir. Crit. Care Med.* **164,** 2213–2219
15. Dussurget, O., Stewart, G., Neyrolles, O., Pescher, P., Young, D., and Marchal, G. (2001) Role of *Mycobacterium tuberculosis* copper-zinc superoxide dismutase. *Infect. Immun.* **69,** 529–533
16. Smith, I. (2003) Mycobacterium tuberculosis pathogenesis and molecular determinants of virulence. *Clin. Microbiol. Rev.* **16,** 463–496
17. Bunting, K., Cooper, J. B., Badasso, M. O., Tickle, I. J., Newton, M., Wood, S. P., Zhang, Y., and Young, D. (1998) Engineering a change in metal-ion specificity of the iron-dependent superoxide dismutase from *Mycobacterium tuberculosis* x-ray structure analysis of site-directed mutants. *Eur. J. Biochem.* **251,** 795–803
18. Braunstein, M., Espinosa, B. J., Chan, J., Belisle, J. T., and Jacobs, W. R., Jr. (2003) SecA2 functions in the secretion of superoxide dismutase A and in the virulence of *Mycobacterium tuberculosis*. *Mol. Microbiol.* **48,** 453–464
19. Argüello, J. M., Eren, E., and González-Guerrero, M. (2007) The structure and function of heavy metal transport P_{1B}-ATPases. *Biometals* **20,** 233–248
20. Argüello, J. M. (2003) Identification of ion-selectivity determinants in heavy-metal transport P_{1B}-type ATPases. *J. Membr. Biol.* **195,** 93–108
21. González-Guerrero, M., Eren, E., Rawat, S., Stemmler, T. L., and Argüello, J. M. (2008) Structure of the two transmembrane Cu^{+} transport sites of

the Cu^+-ATPases. *J. Biol. Chem.* **283,** 29753–29759
22. Raimunda, D., Subramanian, P., Stemmler, T., and Argüello, J. M. (2012) A tetrahedral coordination of Zinc during transmembrane transport by P-type Zn^{2+}-ATPases. *Biochim. Biophys. Acta* **1818,** 1374–1377
23. Zielazinski, E. L., Cutsail, G. E., 3rd, Hoffman, B. M., Stemmler, T. L., and Rosenzweig, A. C. (2012) Characterization of a cobalt-specific P_{1B}-ATPase. *Biochemistry* **51,** 7891–7900
24. Sassetti, C. M., and Rubin, E. J. (2003) Genetic requirements for mycobacterial survival during infection. *Proc. Natl. Acad. Sci. U.S.A.* **100,** 12989–12994
25. Talaat, A. M., Lyons, R., Howard, S. T., and Johnston, S. A. (2004) The temporal expression profile of *Mycobacterium tuberculosis* infection in mice. *Proc. Natl. Acad. Sci. U.S.A.* **101,** 4602–4607
26. Tailleux, L., Waddell, S. J., Pelizzola, M., Mortellaro, A., Withers, M., Tanne, A., Castagnoli, P. R., Gicquel, B., Stoker, N. G., Butcher, P. D., Foti, M., and Neyrolles, O. (2008) Probing host pathogen cross-talk by transcriptional profiling of both *Mycobacterium tuberculosis* and infected human dendritic cells and macrophages. *PLoS One* **3,** e1403
27. Calder, K. M., and Horwitz, M. A. (1998) Identification of iron-regulated proteins of *Mycobacterium tuberculosis* and cloning of tandem genes encoding a low iron-induced protein and a metal transporting ATPase with similarities to two-component metal transport systems. *Microb. Pathog.* **24,** 133–143
28. Edgar, R. C. (2004) MUSCLE. Multiple sequence alignment with high accuracy and high throughput. *Nucleic Acids Res.* **32,** 1792–1797
29. Hall, T. A. (1999) BioEdit. A user-friendly biological sequence alignment editor and analysis program for Windows 95/98/NT. *Nucleic Acids Symp. Ser.* **41,** 95–98
30. Gouet, P., Courcelle, E., Stuart, D. I., and Métoz, F. (1999) ESPript. Analysis of multiple sequence alignments in PostScript. *Bioinformatics* **15,** 305–308
31. Kim, R., Sandler, S. J., Goldman, S., Yokota, H., Clark, A. J., and Kim, S.-H. (1988) Overexpression of archaeal proteins in. *Escherichia coli*. *Biotechnol. Lett.* **20,** 207–210
32. Rensing, C., Mitra, B., and Rosen, B. P. (1997) The *zntA* gene of *Escherichia coli* encodes a Zn(II)-translocating P-type ATPase. *Proc. Natl. Acad. Sci. U.S.A.* **94,** 14326–14331
33. Mandal, A. K., Cheung, W. D., and Argüello, J. M. (2002) Characterization of a thermophilic P-type Ag^+/Cu^+-ATPase from the extremophile *Archaeoglobus fulgidus*. *J. Biol. Chem.* **277,** 7201–7208
34. Bradford, M. M. (1976) A rapid and sensitive method for the quantitation of microgram quantities of protein utilizing the principle of protein-dye binding. *Anal. Biochem.* **72,** 248–254
35. Lanzetta, P. A., Alvarez, L. J., Reinach, P. S., and Candia, O. A. (1979) An improved assay for nanomole amounts of inorganic phosphate. *Anal. Biochem.* **100,** 95–97
36. Raimunda, D., Long, J. E., Sassetti, C. M., and Argüello, J. M. (2012) Role in metal homeostasis of CtpD, a Co^{2+} transporting P_{1B4}-ATPase of *Mycobacterium smegmatis*. *Mol. Microbiol.* **84,** 1139–1149
37. van Kessel, J. C., and Hatfull, G. F. (2007) Recombineering in *Mycobacterium tuberculosis*. *Nat. Methods* **4,** 147–152
38. Griffin, J. E., Pandey, A. K., Gilmore, S. A., Mizrahi, V., McKinney, J. D., Bertozzi, C. R., and Sassetti, C. M. (2012) Cholesterol catabolism by *Mycobacterium tuberculosis* requires transcriptional and metabolic adaptations. *Chem. Biol.* **19,** 218–227
39. Guinn, K. M., Hickey, M. J., Mathur, S. K., Zakel, K. L., Grotzke, J. E., Lewinsohn, D. M., Smith, S., and Sherman, D. R. (2004) Individual RD1-region genes are required for export of ESAT-6/CFP-10 and for virulence of. *Mycobacterium tuberculosis*. *Mol. Microbiol.* **51,** 359–370
40. De Groote, M. A., Ochsner, U. A., Shiloh, M. U., Nathan, C., McCord, J. M., Dinauer, M. C., Libby, S. J., Vazquez-Torres, A., Xu, Y., and Fang, F. C. (1997) Periplasmic superoxide dismutase protects *Salmonella* from products of phagocyte NADPH-oxidase and nitric oxide synthase. *Proc. Natl. Acad. Sci. U.S.A.* **94,** 13997–14001
41. González-Guerrero, M., Raimunda, D., Cheng, X., and Argüello, J. M. (2010) Distinct functional roles of homologous Cu^+ efflux ATPases in *Pseudomonas aeruginosa*. *Mol. Microbiol.* **78,** 1246–1258
42. Livak, K. J., and Schmittgen, T. D. (2001) Analysis of relative gene expression data using real-time quantitative PCR and the $2^{-\Delta\Delta}C_T$ method. *Methods* **25,** 402–408
43. Beauchamp, C., and Fridovich, I. (1971) Superoxide dismutase. Improved assays and an assay applicable to acrylamide gels. *Anal. Biochem.* **44,** 276–287
44. Sharma, R., Rensing, C., Rosen, B. P., and Mitra, B. (2000) The ATP hydrolytic activity of purified ZntA, a Pb(II)/Cd(II)/Zn(II)-translocating ATPase from *Escherichia coli*. *J. Biol. Chem.* **275,** 3873–3878
45. Tsai, K. J., and Linet, A. L. (1993) Formation of a phosphorylated enzyme intermediate by the cadA Cd^{2+}-ATPase. *Arch. Biochem. Biophys.* **305,** 267–270
46. Fan, B., and Rosen, B. P. (2002) Biochemical characterization of CopA, the *Escherichia coli* Cu(I)-translocating P-type ATPase. *J. Biol. Chem.* **277,** 46987–46992
47. Scherer, J., and Nies, D. H. (2009) CzcP is a novel efflux system contributing to transition metal resistance in *Cupriavidus metallidurans* CH34. *Mol. Microbiol.* **73,** 601–621
48. Yamakura, F., Kobayashi, K., Tagawa, S., Morita, A., Imai, T., Ohmori, D., and Matsumoto, T. (1995) pH-dependent activity change of superoxide dismutase from *Mycobacterium smegmatis*. *Biochem. Mol. Biol. Int.* **36,** 233–240
49. Papp-Wallace, K. M., and Maguire, M. E. (2006) Manganese transport and the role of manganese in virulence. *Annu. Rev. Microbiol.* **60,** 187–209
50. Gregory, E. M., and Dapper, C. H. (1983) Isolation of iron-containing superoxide dismutase from *Bacteroides fragilis*. Reconstitution as a Mn-containing enzyme. *Arch. Biochem. Biophys.* **220,** 293–300
51. Meier, B., Sehn, A. P., Schininà, M. E., and Barra, D. (1994) *In vivo* incorporation of copper into the iron-exchangeable and manganese-exchangeable superoxide-dismutase from *Propionibacterium shermanii*. Amino acid sequence and identity of the protein moieties. *Eur. J. Biochem.* **219,** 463–468
52. Meier, B., Barra, D., Bossa, F., Calabrese, L., and Rotilio, G. (1982) Synthesis of either Fe- or Mn-superoxide dismutase with an apparently identical protein moiety by an anaerobic bacterium dependent on the metal supplied. *J. Biol. Chem.* **257,** 13977–13980
53. Hingley-Wilson, S. M., Sambandamurthy, V. K., and Jacobs, W. R., Jr. (2003) Survival perspectives from the world's most successful pathogen, *Mycobacterium tuberculosis*. *Nat. Immunol.* **4,** 949–955
54. Chackerian, A. A., Alt, J. M., Perera, T. V., Dascher, C. C., and Behar, S. M. (2002) Dissemination of *Mycobacterium tuberculosis* is influenced by host factors and precedes the initiation of T-cell immunity. *Infect. Immun.* **70,** 4501–4509
55. Dutta, S. J., Liu, J., Stemmler, A. J., and Mitra, B. (2007) Conservative and nonconservative mutations of the transmembrane CPC motif in ZntA. Effect on metal selectivity and activity. *Biochemistry* **46,** 3692–3703
56. Okkeri, J., and Haltia, T. (2006) The metal-binding sites of the zinc-transporting P-type ATPase of *Escherichia coli*. Lys^{693} and Asp^{714} in the seventh and eighth transmembrane segments of ZntA contribute to the coupling of metal binding and ATPase activity. *Biochim. Biophys. Acta* **1757,** 1485–1495
57. Checa, S. K., Espariz, M., Audero, M. E., Botta, P. E., Spinelli, S. V., and Soncini, F. C. (2007) Bacterial sensing of and resistance to gold salts. *Mol. Microbiol.* **63,** 1307–1318
58. Rensing, C., Sun, Y., Mitra, B., and Rosen, B. P. (1998) Pb(II)-translocating P-type ATPases. *J. Biol. Chem.* **273,** 32614–32617
59. Grover, A., and Sharma, R. (2006) Identification and characterization of a major Zn(II) resistance determinant of. *Mycobacterium smegmatis*. *J. Bacteriol.* **188,** 7026–7032
60. Grass, G., Fan, B., Rosen, B. P., Franke, S., Nies, D. H., and Rensing, C. (2001) ZitB (YbgR), a member of the cation diffusion facilitator family, is an additional zinc transporter in *Escherichia coli*. *J. Bacteriol.* **183,** 4664–4667
61. Maciag, A., Dainese, E., Rodriguez, G. M., Milano, A., Provvedi, R., Pasca, M. R., Smith, I., Palù, G., Riccardi, G., and Manganelli, R. (2007) Global analysis of the *Mycobacterium tuberculosis* Zur (FurB) regulon. *J. Bacteriol.* **189,** 730–740
62. Faulkner, M. J., and Helmann, J. D. (2011) Peroxide stress elicits adaptive

changes in bacterial metal ion homeostasis. *Antioxid. Redox Signal.* **15,** 175–189
63. Jacobsen, F. E., Kazmierczak, K. M., Lisher, J. P., Winkler, M. E., and Giedroc, D. P. (2011) Interplay between manganese and zinc homeostasis in the human pathogen *Streptococcus pneumoniae*. *Metallomics* **3,** 38–41
64. Thakur, K. G., Praveena, T., and Gopal, B. (2010) Structural and biochemical bases for the redox sensitivity of *Mycobacterium tuberculosis* RslA. *J. Mol. Biol.* **397,** 1199–1208
65. Suzuki, Y. J., Forman, H. J., and Sevanian, A. (1997) Oxidants as stimulators of signal transduction. *Free Radic. Biol. Med.* **22,** 269–285
66. Gold, B., Deng, H., Bryk, R., Vargas, D., Eliezer, D., Roberts, J., Jiang, X., and Nathan, C. (2008) Identification of a copper-binding metallothionein in pathogenic mycobacteria. *Nat. Chem. Biol.* **4,** 609–616
67. Achard-Joris, M., Moreau, J. L., Lucas, M., Baudrimont, M., Mesmer-Dudons, N., Gonzalez, P., Boudou, A., and Bourdineaud, J. P. (2007) Role of metallothioneins in superoxide radical generation during copper redox cycling. Defining the fundamental function of metallothioneins. *Biochimie* **89,** 1474–1488
68. Harth, G., and Horwitz, M. A. (1999) Export of recombinant *Mycobacterium tuberculosis* superoxide dismutase is dependent upon both information in the protein and mycobacterial export machinery. A model for studying export of leaderless proteins by pathogenic mycobacteria. *J. Biol. Chem.* **274,** 4281–4292

A Novel P_{1B}-type Mn^{2+}-transporting ATPase Is Required for Secreted Protein Metallation in Mycobacteria

Teresita Padilla-Benavides, Jarukit E. Long, Daniel Raimunda, Christopher M. Sassetti and José M. Argüello

J. Biol. Chem. 2013, 288:11334-11347.
doi: 10.1074/jbc.M112.448175 originally published online March 12, 2013
